In Vitro Investigation on Poly(lactide)−Tween 80 Copolymer Nanoparticles Fabricated by Dialysis Method for Chemotherapy

Zhiping Zhang† and Si-Shen Feng*,†,‡

Department of Chemical & Biomolecular Engineering and Division of Bioengineering, Faculty of Engineering, National University of Singapore, 10 Kent Ridge Crescent, Singapore 119260

Received December 15, 2005; Revised Manuscript Received January 23, 2006

Polysorbate 80 (Tween 80) has been widely used as an emulsifier with excellent effects in nanoparticles technology for biomedical applications. This work was thus triggered to synthesize poly(lactide)/Tween 80 copolymers with various copolymer blend ratio, which were synthesized by ring-opening polymerization and characterized by ^{1}H NMR and TGA. Nanoparticles of poly(lactide)/Tween 80 copolymers were prepared by the dialysis method without surfactants/emulsifiers involved. Paclitaxel was chosen as a prototype anticancer drug due to its excellent therapeutic effects against a wide spectrum of cancers. The drug-loaded nanoparticles of poly(lactide)/Tween 80 copolymers were then characterized by various state-of-the-art techniques, including laser light scattering for particles size and size distribution, field emission scanning electron microscopy (FESEM) and atomic force microscopy (AFM) for surface morphology; laser Doppler anemometry for zeta potential; differential scanning calorimetry (DSC) for the physical status of the drug encapsulated in the polymeric matrix; X-ray photoelectron spectrometer (XPS) for surface chemistry; high performance liquid chromatography (HPLC) for drug encapsulation efficiency; and in vitro drug release kinetics. HT-29 cells and Glioma C6 cells were used as an in vitro model of the GI barrier for oral chemotherapy and a brain cancer model to evaluate in vitro cytotoxicity of the paclitaxel-loaded nanoparticles. The viability of C6 cells was decreased from 37.4 ± 4.0% for poly(D,L-lactide-*co*-glycolic acid) (PLGA) nanoparticles to 17.8 ± 4.2% for PLA−Tween 80−10 and 12.0 ± 5.4% for PLA-Tween 80−20 copolymer nanoparticles, which was comparable with that for Taxol at the same 50 μg/mL drug concentration.

1. Introduction

Nanoparticles of biodegradable polymers for anticancer drug delivery have attracted intensive interest in recent years because nanoparticles can provide a sustained, controlled, and targeted delivery as drug carriers and thus lead to high therapeutic efficiency and low side effects. However, nanoparticles could be rapidly eliminated/excreted by the macrophages in the reticuloendothelial system (RES) located mainly in the liver and spleen and resulted in short half-life in the blood system after intravenously administrated.[1] To achieve long blood circulation time to avoid or minimize the absorption of nanoparticles onto the phagocytes, several attempts were made.[2] Physicochemical studies have shown that coating nanoparticles with a neutral hydrophilic layer can generate stealth particles and decrease the phagocytic uptake and thus significantly increase the blood circulation time and high level of drug concentration in non-RES organs such as intestine, kidney, etc.[3,4] A number of surfactants such as poloxamers, poloxamines,[3] poly(ethylene glycol) (PEG),[5] and Tween 80[6−8] were chosen as the coating materials. Poloxamer 407- or poloxamine 908-coated poly(D,L-lactide-*co*-glycolic acid) (PLGA) nanoparticles have been found to increase the circulation time and decrease liver and spleen accumulation of incorporated radiolabeled indium-111-oxinie.[3] Moreover, to apply nanoparticles as carriers to cross the gastrointestinal (GI) barrier and the blood brain barrier (BBB), some other coating surfactants were also considered. Dong and Khin used montmorillonite (MMT) and TPGS (D-α-tocopheryl poly(ethylene glycol) 1000 succinate) coated nanoparticles for oral chemotherapy and found that the coated nanoparticles can enhance cellular uptake of the nanoparticles by Caco-2 cells and HT-29 cells and thus high cytotoxicity of the encapsulated drugs.[9,10] Polysorbate 80 (Tween 80) coated nanoparticles have been reported to have the capability to transport the loaded drugs across BBB after intravenous administration.[11−13] This may be because the nanoparticles can adsorb apoliproprotein E (ApoE), which mimics low-density lipoprotein (LDL), onto the nanoparticle surface and thus be uptaken by the brain capillary endothelial cells via receptor-mediated endocytosis.[14−18] Gulyaev found that Tween 80-coated poly(butyl cyanoacrylate) nanoparticles can achieve about 60-fold brain concentration of administrated doxorubicin.[19,20] Tween 80 is a polyethylene sorbitol ester with a molecular weight of 1310 Da. Tween 80 has been widely used in solubilizing proteins and isolating nuclei from cells. It is widely used as an emulsifier/surfactant/stabilizer in the fabrication of polymeric nanoparticles, liposomes, or solid lipid nanoparticles.[21−23]

However, the absorbed polymer on the surface of the nanoparticles might be desorbed in vivo because of replacement by the blood components with high affinity to the particles surface.[24] To increase stability of the coated polymer on the surface of nanoparticles, copolymers of similar surface properties such as PLA−MPEG (polylactide−methoxyl poly(ethylene glycol)),[25−27] PLA−PEG−PLA,[28,29] PCL−Pluronic F127−PCL,[30] and PLA−TPGS[31] were synthesized. These copolymers demonstrated amphiphilic structure with PEG, TPGS, and F127 on the surface of nanoparticles, which can have better performance for drug delivery.

In this present study, PLA−Tween 80 copolymers were synthesized in the presence of lactide and Tween 80 as

* Corresponding author. Tel: (65) 6516-3835. Fax: (65) 6779-1936. E-mail: chefss@nus.edu.sg.
† Department of Chemical & Biomolecular Engineering.
‡ Division of Bioengineering.

10.1021/bm050953v CCC: $33.50
Published on Web 03/23/2006

monomers and stannous octoate as catalyst. The synthesized copolymers were characterized by ^{1}H NMR for structure and thermogravimetric analysis for mass ratios between Tween 80 and PLA in the copolymers and polymer thermal property. Paclitaxel was used as prototype drug because of its excellent therapeutic effects against a wide spectrum of cancers including breast cancer, ovarian cancer, colon cancer, small and nonsmall cell lung caner, neck cancer, and AIDS-related Kaposi's sarcoma.[32−35] To avoid side effects caused by the adjuvant Cremophor EL used in the current clinical formulation of paclitaxel,[36−40] paclitaxel-loaded nanoparticles of PLA-Tween 80 copolymers were fabricated by the dialysis method, which can be much simpler than, and avoid side effects of, the surfactants used in the traditional solvent extraction/evaporation method.[41−43] The drug-loaded nanoparticles were characterized by laser light scattering for particles size and size distribution; field emission scanning electron microscopy (FESEM) and atomic force microscopy (AFM) for surface morphology; laser doppler anemometry for zeta potential; differential scanning calorimetry (DSC) for the physical status of the drug encapsulated in the polymeric matrix; X-ray photoelectron spectrometer (XPS) for surface chemistry; high performance liquid chromatography (HPLC) for drug encapsulation efficiency and in vitro drug release kinetics. HT-29 cells, a human colon carcinoma cell line, and Glioma C6 cells were used as an in vitro model of the GI barrier for oral chemotherapy and a brain cancer model, respectively, to evaluate in vitro cytotoxicity of paclitaxel-loaded nanoparticles. The preliminary results showed a great potential of PLA−Tween 80 copolymer nanoparticles for cancer chemotherapy.

2. Materials and Methods

2.1. Materials. Paclitaxel was purchased from Dabur India Limited, India. PLGA (50:50) with L/G molar ratio of 50:50 (Mw 40 000−75 000), stannous octoate, 3-(4,5-cimethylthiazol-2-yl)-2,5-diphenyl tetrazolium bromide (MTT), penicillin-streptomycin solution, and Trypsin-EDTA solution were purchased from Sigma (St. Louis, MO). Fetal bovine serum (FBS) was received from Gibco (Life Technologies, AG, Switzerland). Tween-80 (Polyoxyethylene Sorbitan Monooleate) from Sigma was dried overnight under vacuum before use. Lactide (3,6-dimethyl-1,4-dioxane-2,5-dione) was purchased from Aldrich and recrystallized twice in ethyl acetate. All solvents used are of HPLC grade, which include ethyl acetate from Merck, dichloromethane (DCM) and acetonitrile from Aldrich, and *N*,*N*-dimethylformamide (DMF) from Tedia.

2.2. Synthesis of PLA-Tween 80 Copolymers. Appropriate amounts of lactide, Tween 80, and 0.5 wt % stannous octoate (in distilled toluene) were added to a glass ampule, which was dipped into liquid nitrogen. The mixture was degassed by four vacuum-purge cycles with nitrogen. The ampule was sealed with a butane burner under vacuum condition and allowed to react at 145 °C for 12 h. The cooled product was dissolved in DCM and then precipitated twice in 15-fold volume of methanol. The precipitant was subsequently separated by filtration and vacuum-dried for 2 days at 45 °C.

2.3. Copolymer Characterization. Nuclear magnetic resonance (NMR, 300 MHz ^{1}H NMR, Bruker ACF 300) was deployed to determine the structure, number-average molecular weight, and the Tween 80 content of the copolymers. Thermogravimetric analysis (TGA, TGA 2050 thermogravimetric analyzer, USA) was carried out to investigate the thermal properties of the copolymers. A total of 10−15 mg of the copolymer was weighed into a heating pan and heated from 25 to 500 °C at a rate of 10 °C/min. A steady flow of nitrogen gas was supplied to the furnace. From the results given by TGA, the composition and hence molecular weight of the various copolymers can be calculated. Biodegradation studies of the copolymers were performed in PBS at 37 °C. Briefly, 10.0 mg of the freeze-dried sample was placed in 1.5 mL of PBS in a water bath. Periodically, the samples were taken out from the water bath and centrifugation was carried out at a speed of 11 500 rpm for 30 min. The supernatant was discarded, and the remaining polymer was freeze-dried. After that, the sample was weighed, and the percentage of remaining polymer weight was plotted against time.

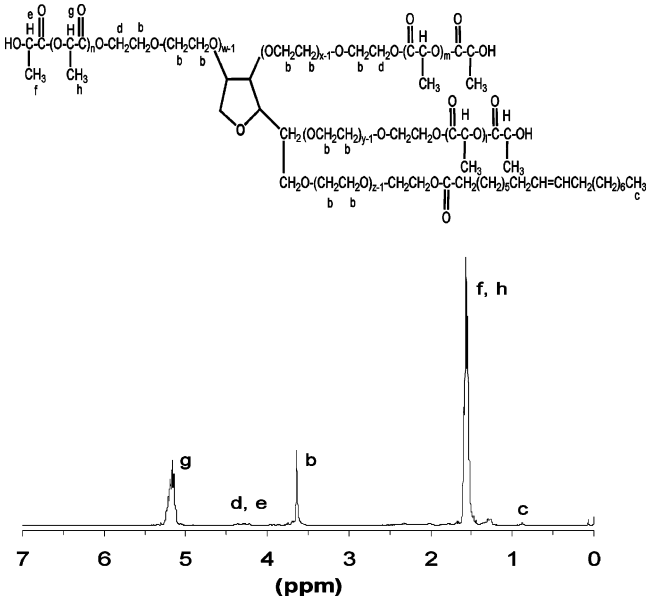

Figure 1. Typical ^{1}H NMR spectra of PLA-Tween 80 copolymers in $CDCl_3$.

Table 1. Composition and Molecular Weight of PLA−Tween 80 Copolymers

	Tween 80 composition (%)			yield	M_n[a]
copolymers	theor.	^{1}H NMR	TGA	(%)	(^{1}H NMR)
PLA−Tween 80−10	10.0	8.5	6.6	83.7	15, 500
PLA−Tween 80−20	20.0	15.3	14.3	85.2	8, 560

[a] Determined by the integration ratio of peak at 5.2 ppm to 3.65 ppm.

Table 2. Size, Zeta Potential and Drug Encapsulation Efficiency of Paclitaxel-Loaded Nanoparticles Fabricated from Different Copolymers

polymers	particle size (nm)	zeta potential (mv)	encapsulation efficiency (%)[b]	yield (%)
PLA−Tween 80−10	171 ± 28	−20.4 ± 1.5	65.8 ± 8.7	56.5
PLA−Tween 80−20	138 ± 15	−15.0 ± 2.1	46.5 ± 2.5	60.0
PLGA50/50	242 ± 13	−20.5 ± 0.8	60.2 ± 6.5	49.8

[b] Drug loading is 6%.

2.4. Fabrication of Paclitaxel-Loaded Nanoparticles. The paclitaxel-loaded nanoparticles of the copolymers were fabricated by the dialysis method. A total of 5 mg of paclitaxel and 45 mg of copolymer were dissolved into 50 mL of DMF and then vortexed for 60 s. The solution was dialyzed for 30 h in a dialysis bag (MWCO 3, 500, Spectrum) in 5 L of water, which was exchanged at intervals of 2−3 h. After dialysis, the resulted suspension in the bag was collected and sonicated before being centrifuged at 11 500 rpm for 20 min. The pellet was redispersed in water and freeze-dried for 2 days to get the nanoparticles powder.

2.5. Nanoparticle Characterization. 2.5.1. Particle Size and Zeta Potential. The particles size and size distribution of the nanoparticles were measured by laser light scattering (Brookhaven Instruments Corporation, 90 Plus). The surface charge of the nanoparticles was determined by zeta potential analyzer (Brookhaven Instruments Corporation, ZetaPlus) in deionized water. A total of 3 mL of the

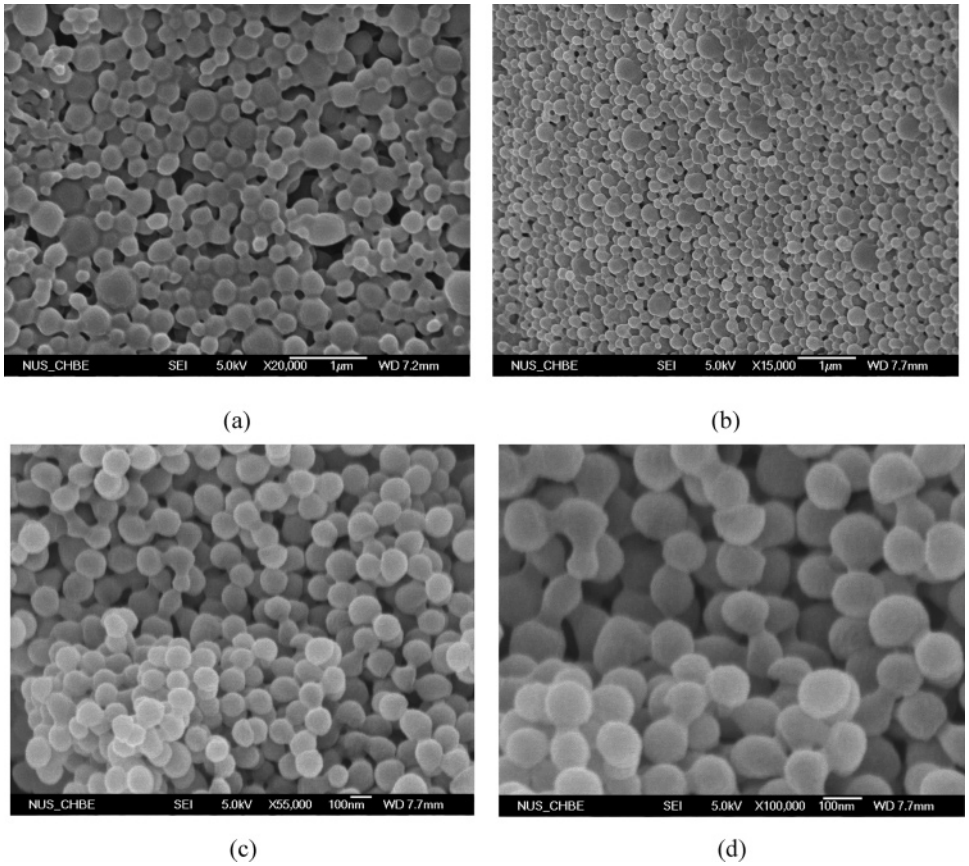

Figure 2. FESEM images of paclitaxel-loaded nanoparticles of (a) PLA−Tween 80−10; (b) PLGA 50/50; (c) PLA−Tween 80−20, 55, 000 magnification; and (d) PLA−Tween 80−20, 100, 000 magnification.

nanoparticle suspension was redispersed by using a sonicator to prevent aggregation of the nanoparticles and then transferred into an acrylic square cell for measurement. A typical result was obtained based on the average from 7 runs.

2.5.2. Surface Morphology. The surface morphology of the nanoparticles was observed by a field emission scanning electron microscopy (FESEM, JEOL, SM-6700F, Japan). Powder samples of the nanoparticles were applied flatly on double-sided sticky tape attached to a metal stub and then coated with a platinum layer by the Auto Fine Platinum Coater (JEOL JFC-1300, Tokyo, Japan) for 50 s under a pressure of 5 Pa and a current intensity of 30 mA. AFM can be used to get 3D images with subnanometer resolution and quantitative measurement of surface roughness without metallization before observation. The surface of the nanoparticles was scanned with Nanoscope IIIa Atomic Force Microscope (Digital Instrument, Santa Barbara, CA) under tapping mode.

2.5.3. Drug Encapsulation Efficiency (EE). Paclitaxel entrapped in the nanoparticles was measured by HPLC (Agilent LC1100 Series, Column: Inertsil ODS-3, pore size 5 μm, 4.6 $\times$ 150 mm, GL science Inc, Tokyo, Japan) at 227 nm UV wavelength. Three milligrams of the paclitaxel-loaded nanoparticles were dissolved in 2 mL DCM under vigorous vortexing. The solution was left for evaporation and then the deposit was dissolved in 3 mL mobile phase (50/50 v/v acetonitrile/water solution). The resulting solution was transferred into a HPLC vial by using a syringe filter (PVDF membrane, 0.45 μm). Drug encapsulation efficiency is a reflection of drug loaded into the nanoparticles against that used during fabrication.

2.5.4. Surface Chemistry. An X-ray photoelectron spectrometer (XPS) (RATOS AXIS HSi system) was used for the analysis of surface composition of the copolymers and the nanoparticles. A survey spectrum covering a binding energy from 0 to 1200 eV was registered by a fixed transmission mode with pass energy of 80 eV. The sample was attached to a glass piece which was then stuck on a metal stub using double-sided sticky tape. After that, the data were extracted and a peak curve fitting was done by using the software provided by the manufacturer.

2.5.5. Thermogram Properties. A total of 5−10 mg of paclitaxel-loaded nanoparticles were weighed and placed into a sealed aluminum pan. The physical status of paclitaxel encapsulated in the nanoparticle matrix was analyzed by using a differential scanning calorimetry (DSC, Mettler Toledo DSC 822e). The sample was purged with 40 mL/min of dry nitrogen and heated from 0 to 250 °C at a rate of 10 °C/min. Indium was used as the standard reference material for the temperature and energy scale calibration.

2.5.6. In Vitro Drug Release. A total of 1 mg of drug-loaded nanoparticles was suspended into 2 mL of PBS solution with 0.1% w/v Tween 80 at pH 7.4 in a centrifuge tube, which is put in an orbital water bath shaking at 120 rpm at 37.2 °C. Each batch of samples was measured in triplicate. Tween 80 was used to increase the solubility of paclitaxel in buffer solution and avoid the binding of paclitaxel to the tube surface. At the designated moments, the tube was taken out from the water bath, and centrifugation was carried out at a speed of 11 500 rpm for 20 min. The supernatant was transferred into a screw capped tube. The solution was extracted with 1 mL of DCM and reconstituted in 1 mL of the mobile phase. The analysis procedure was similar as the measurement of EE. The pellet was resuspended in 2 mL of fresh release medium and then placed back in the water bath shaker for continuous measurement.

2.6. In Vitro Cytotoxicity. In this study, in vitro cancer cell viability was accessed by a MTT toxic assay, which is widely used to evaluate the cytotoxic activity of drugs or biomaterials. This method is based on the cellular reductive capacity of living cells to metabolize the yellow tetrazolium salt, MTT, to a chromophore, formazan product, whose absorbance can be determined by spectrophotometric measurement. Human colon adenocarcinoma cells (HT-29, passages 25−30) and C6 glioma cells (passage 6−10) (American Type Culture Collection,VA) were used for in vitro cytotoxicity evaluation of the paclitaxel-loaded nanoparticles in comparison with paclitaxel formulated in Cremophor EL (Taxol). The cells were cultured in 20 mL of DMEM medium supplemented with 10% FBS and 1% antibiotic-antimycotic in a 75

cm^2 culture flask. The culture flask was incubated at 37 °C in humidified environment containing 5% CO_2. The medium was replenished every other day until confluency was reached. The cells were harvested with 0.125% of Trypsin-EDTA solution and seeded in 96-well transparent plates (Costar, Corning, NY) at 4×10^4 cells/well.

When the cells seeded in 96-well transparent plates are about 70% confluent, the culture medium in the wells was replaced with 100 μL of the drug loaded nanoparticle suspension or Taxol in fresh medium with the drug concentration ranging from 0.025 to 50 μg/mL for 24 and 72 h incubation. The drug-loaded nanoparticles were sterilized by gama-irradiation before the cytotoxicity test. Six wells were used for each nanoparticl sample or Taxol. One row of 12 wells was used as a positive control, in which only culture medium was added to the wells. At the designated times, the medium containing the drug was removed and the cells are washed twice with 50 μL of PBS. After removal of the PBS, 90 μL of culture medium and 10 μL of MTT were added to each of the wells. The cells were then incubated for 3−4 h and the solution was then removed from the precipitate. A total of 100 mL of 2-propanol was added to the wells and the level of absorbance was measured by using a microplate reader. The cell viability was calculated as

$$\text{cell viability} = \frac{\text{Abs}_s}{\text{Abs}_{\text{control}}} \times 100\% \qquad (1)$$

where Abs_s is the absorbance of the cells incubated with different drug formulations and $\text{Abs}_{\text{control}}$ is the absorbance of the control cells. Statistical evaluation was analyzed by using Student's *t*-test.

3. Results and Discussion

3.1. Synthesis of PLA-Tween 80 Copolymers. PLA-Tween 80 copolymers were synthesized by ring opening polymerization in the presence of lactide and Tween 80. The synthesis process is similar to that we developed earlier for synthesis of the PLA−TPGS copolymer.[31] The PLA-Tween 80 copolymer was characterized by ^{1}H NMR in $CDCl_3$ and the spectrum is shown in Figure 1. The signals at 4.30 ppm indicated the successful synthesis of the PLA-Tween 80 copolymer. No signals of the methane proton of the PLA−O-*CH*(CH_3)-COOH group appeared at 4.9−5.0 ppm, which demonstrated that there was negligible or no PLA homopolymer in the synthesized copolymer.[44] The peaks at 5.2 and 1.60 ppm were assigned to the −CH protons and methyl protons $-CH_3$ of the PLA segment, respectively. The peak at 3.65 ppm could be attributed to the $-CH_2$ protons of the PEO part of Tween 80 in the copolymers. The small peaks in the aliphatic region belong to various moieties $-CH_3$ and $-CH_2$ protons of the Tween 80 tails. The lactide monomer peak at 5.1 ppm was not detected, which demonstrated that the precipitation process in treatment of the copolymer product can remove the lactide monomer thoroughly.

The number average molecular weight and Tween 80 composition in the copolymers calculated from NMR were shown in Table 1. The molecular weight was determined by the integration ratio of the peak at 5.2 and 3.65 ppm. PLA−Tween 80 copolymers showed a biphasic profile of thermogravimetric degradation with an onset temperature of 206 °C for the PLA segment and 374 °C for the Tween 80 segment, which are different from a single mass lost for the Tween 80 monomer (figure not shown). TGA was proposed as a convenient method for evaluating mass ratios of PLA−Tween 80 copolymers, and the results are shown in Table 1. The Tween 80 composition calculated from TGA can match well with NMR results.

3.2. Particles Size, Zeta Potential, and Drug Encapsulation Efficiency. The physicochemical characteristics of paclitaxel-loaded nanoparticles of PLA−Tween 80 copolymers were summarized in Table 2. The PLA−Tween 80 nanoparticles have sizes less than 200 nm in diameter, whereas the size of PLGA

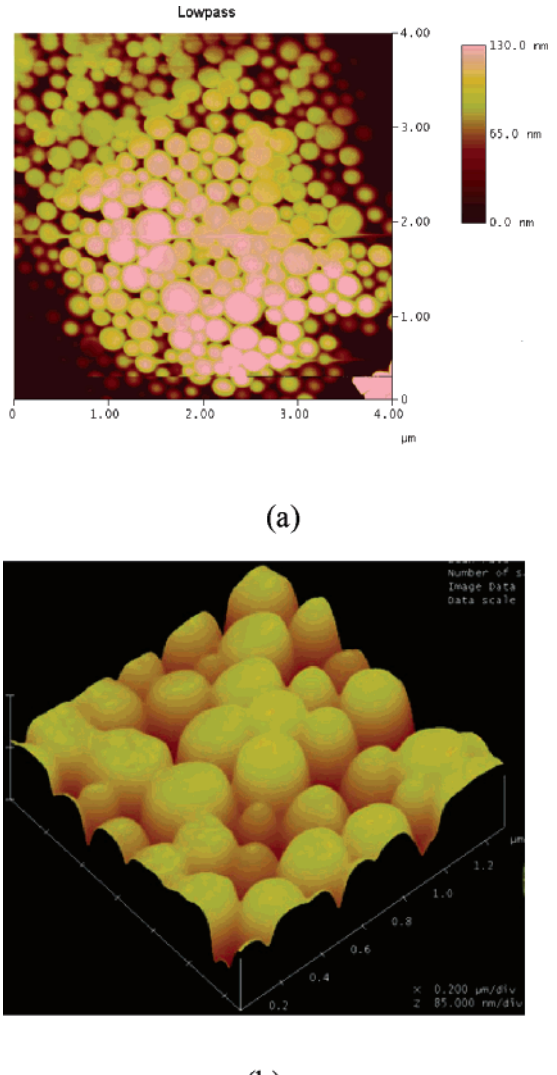

Figure 3. AFM images of paclitaxel-loaded PLA−Tween 80−10 nanoparticles (a) 4 μm × 4 μm 2D image and (b) a zoom-in 3D image.

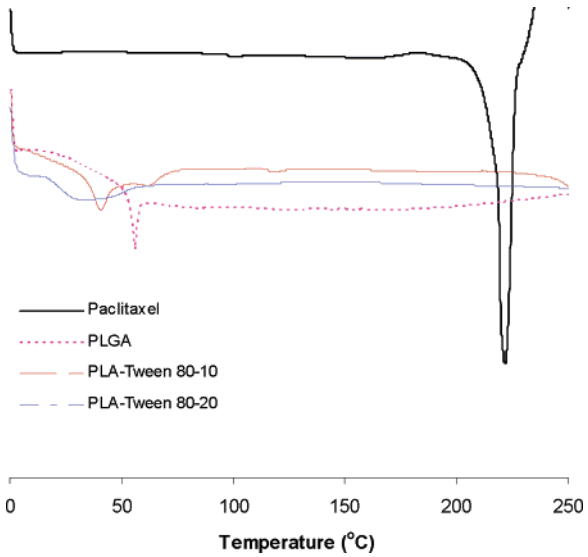

Figure 4. DSC thermograms of paclitaxel and paclitaxel loaded copolymer nanoparticles.

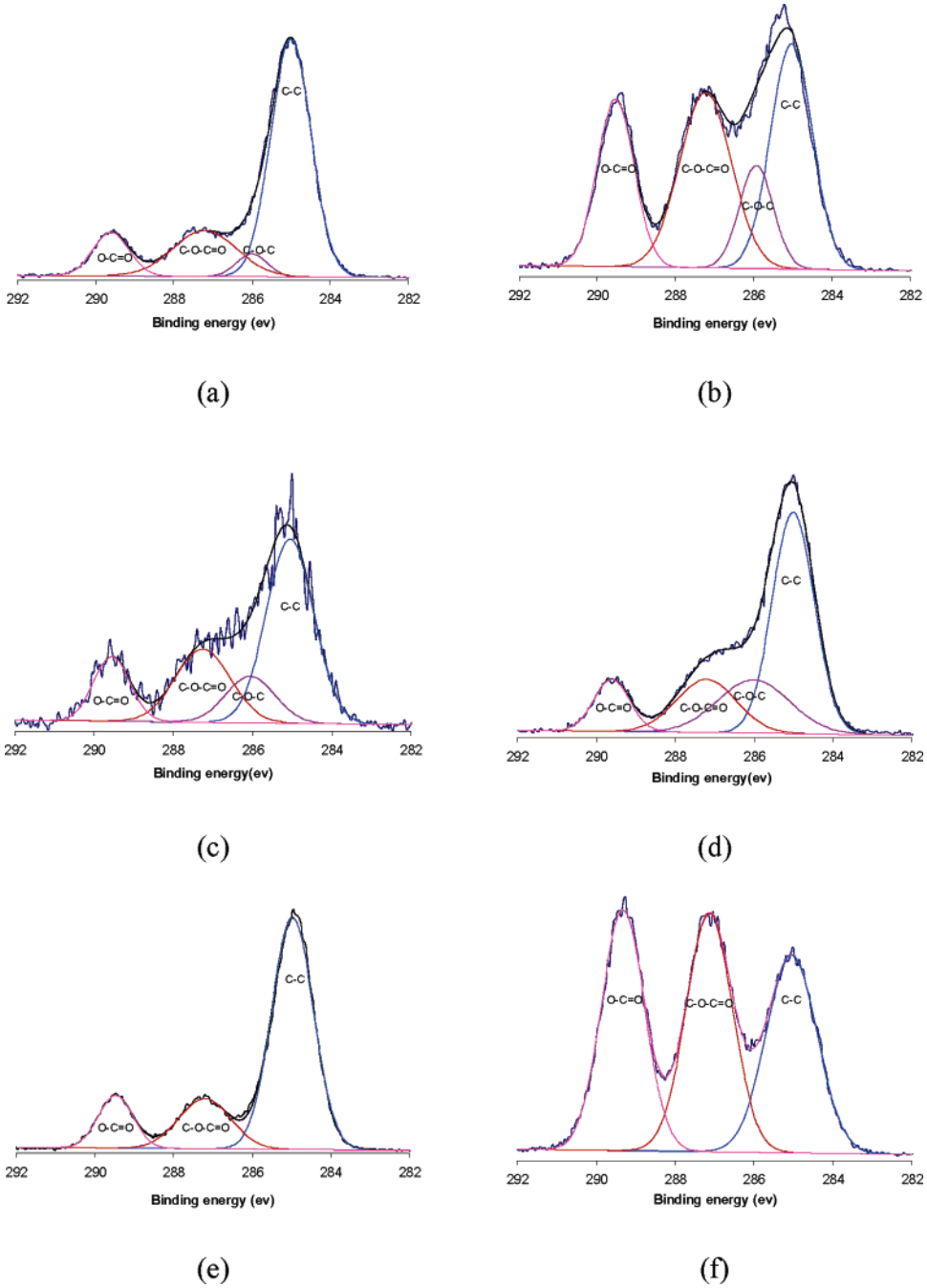

Figure 5. XPS spectra of (a) PLA−Tween 80−10 copolymer; (b) PLA−Tween 80−10 copolymer nanoparticles; (c) PLA−Tween 80−20 copolymer; (d) PLA−Tween 80−20 copolymer nanoparticles; (e) PLGA 50:50; and (f) PLGA 50:50 nanoparticles.

nanoparticles was around 240 nm. Particles size is a crucial parameter in determining in vitro drug release, in vitro cellular uptake, and cancer cell mortality of the nanoparticles as well as in vivo pharmacokinetics and biodistribution and thus the therapeutic effects of the encapsulated drug.[10,42] Nanoparticles less than 200 nm can prevent spleen filtering.[45] Due to the porosity of the tumor vasculature (the effective mean pore size of most peripheral human tumors is about 400 nm) and the lack of lymphatic drainage, colloidal nanoparticles are preferentially distributed in the tumors by the EPR (enhanced permeability and retention) effect.[46] Particles can bypass the P-gp efflux system by small size (preferably 120−200 nm).[47] It can be seen from Table 2 that as the molecular weights of the copolymers decrease, the size and encapsulation efficiency of the nanoparticles were decreased. This may be because the lower the molecular weight of the copolymer is, the lower the hydrophobic interaction between the PLA block chain and the hydrophobic drug, paclitaxel, can result.[45] PLA−Tween 80 nanoparticles can achieve around 60% drug encapsulation efficiency for 6% drug loading. The drug-loaded nanoparticles showed a negative surface charge of around −20 mV. The zeta potential has been used as an index of the nanoparticle stability in the suspension. It can greatly affect the particles stability in suspension through the electronic repulsion between particles. As a result, a higher absolute value of the zeta potential indicates a more stable suspension, and a lower value implicates colloid instability, which could lead to aggregation of nanoparticles.[48] Optimization of the nanoparticles fabrication was also pursued in this research. Nanoparticles fabricated with 1,4-dioxane showed more than a 100 nm larger size than those fabricated with DMF as the

solvent. Although the former process had 10−15% higher drug encapsulation efficiency than the latter, we chose DMF as the solvent since the resulting nanoparticle size was as desired.

3.3. Surface Morphology. The surface morphology of the drug-loaded PLA−Tween 80 nanoparticles was examined by FESEM as shown Figure 2. PLA−Tween 80−20 nanoparticles showed smaller size and lower polydispersity (0.04) compared with PLA−Tween 80−10 (0.12) nanoparticles. The nanoparticle size found from the FESEM images tallies with that detected from the laser light scattering. AFM was also used to study the surface morphology of the drug-loaded nanoparticles with higher resolution as shown in Figure 3. AFM images further confirm the FESEM observation. The nanoparticles show spherical in shape and a relatively smooth surface.

3.4. Physical Status of the Drug in Nanoparticles. The physical status of paclitaxel formulated in the polymeric nanoparticles was investigated by differential scanning calorimetry (DSC). The result is shown in Figure 4. Pure paclitaxel shows a melting endothermic peak at 223 °C, whereas no peak is detected at the range from 150 to 250 °C for the paclitaxel-loaded nanoparticles. This demonstrates that paclitaxel formulated in the polymeric nanoparticles existed in an amorphous or disordered crystalline phase or a solid solution state. Moreover, the prepared nanoparticles all exhibited a phase transition that corresponded to the amorphous solid material as the endothermal peaks appeared around 50 °C.[43] PLA−Tween 80 copolymer nanoparticles exhibited a lower glass transition temperature compared with PLGA nanoparticles.

3.5. Surface Chemistry. X-ray photoelectron spectroscopy (XPS) was applied in this research to analyze the atomic composition of the copolymers and the drug-loaded copolymer nanoparticles. A nitrogen signal was used to detect whether paclitaxel stays on the surface or distributes inside of the polymeric nanoparticles. There is no nitrogen signal detected from XPS N1s results (figure not shown) for the paclitaxel-loaded nanoparticles, which demonstrates that paclitaxel was mainly distributed inside of the copolymer nanoparticles. XPS C1s spectra of the paclitaxel-loaded nanoparticles and the copolymers themselves were shown in Figure 5. The peak at binding energy 286.0 eV was regarded as the indicator of the PEG portion of Tween 80 in the PLA−Tween 80 copolymers.[31,49] The peak ratio of the C−O−C bond was increased from 5.7% for the PLA−Tween 80−10 copolymer and 13.1% for the PLA−Tween 80−20 copolymer to 12.3% for the PLA−Tween 80−10 copolymer nanoparticles and 21.0% for the PLA−Tween 80−20 copolymer nanoparticles. This demonstrates the presence of Tween 80 on the surface of the nanoparticles. The XPS results also demonstrate an increasing O−C═O peak ratio for the nanoparticles, which can be seen from Figure 5, panels b, d, and f, for the nanoparticles in comparison with Figure 5, panels a, c, and e, for the copolymers themselves. Such an increase can lead to high negative charge on the nanoparticle surface and thus high stability of the nanoparticles in their suspension.[50]

3.6. In Vitro Drug Release. The in vitro drug release profiles of the paclitaxel-loaded PLA−Tween 80−10, PLA−Tween 80−20, and PLGA nanoparticles are shown in Figure 6a. Paclitaxel-loaded nanoparticles showed an initial burst release of 25.7 ± 3.0%, 26.1 ± 4.0%, and 23.0 ± 3.5% of the encapsulated drug in the first day, and after 21 days, 57.5 ± 3.3%, 62.0 ± 4.2%, and 52.1 ± 4.6% of the encapsulated drug was released from the PLA−Tween 80−10, PLA−Tween 80−20, and PLGA nanoparticles, respectively. The PLA−Tween 80−20 nanoparticles resulted in faster drug release than the PLGA nanoparticles

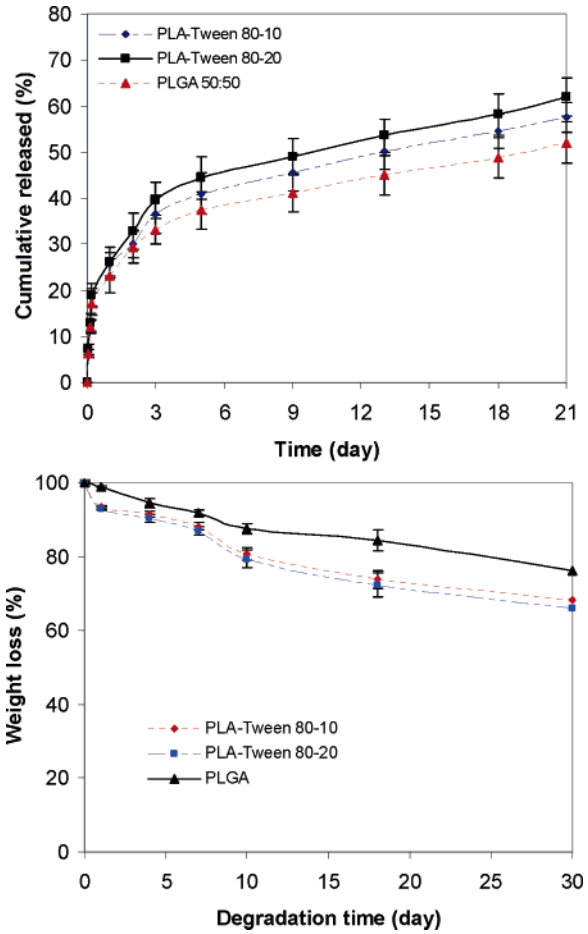

Figure 6. In vitro (a) drug release profile of paclitaxel-loaded copolymers nanoparticles and (b) degradation behavior of copolymers in PBS at 37 °C. Data represents mean ± SD, $n = 3$.

($p < 0.05$) and the higher ratio of Tween 80 in the copolymer composition, the faster the drug was released from the copolymer nanoparticles ($p > 0.05$). The in vitro drug release from nanoparticles is affected by drug diffusion, polymer swelling, polymer erosion, or degradation. The faster drug release may thus be explained by the higher hydrophilicity of the copolymers, which caused the copolymer swell and degrade faster. Indeed, the PLA−Tween 80 copolymer showed a faster degradation rate than the PLGA as can be seen from Figure 6b. After 21 days degradation in PBS, the PLA−Tween 80−20 copolymer showed 33% weight loss compared with 32% for the PLA−Tween 80−10 and 24% for the PLGA.

3.7. In Vitro Cytotoxicity of Paclitaxel-Loaded Nanoparticles. A human colon carcinoma cell line HT-29 as well as a Glioma C6 cell line were used to investigate the cytotoxicity of paclitaxel-loaded nanoparticles of the copolymers, which was compared with that for the commercial formulation Taxol. The drug-loaded nanoparticles were sterilized by gama-radiation for 72 h to exclude the sample contamination effect and were then suspended and cultured with the cells. The measured cytotoxicity was shown in Figure 7, panels a and b, for C6 cells and Figure 7, panels c and d, for HT-29 cells. It can be seen from Figure 7, panels a and b, that paclitaxel-loaded nanoparticles showed higher cell viability compared with Taxol for either 24 or 72 h incubation. Nevertheless, the drug-loaded nanoparticles of PLA−Tween 80−20 copolymer showed much lower cell viability compared with that of PLGA ($p < 0.05$) and PLA−Tween 80−10 copolymer nanoparticles showed comparable cytotoxicity with PLGA nanoparticles ($p > 0.05$). The cell

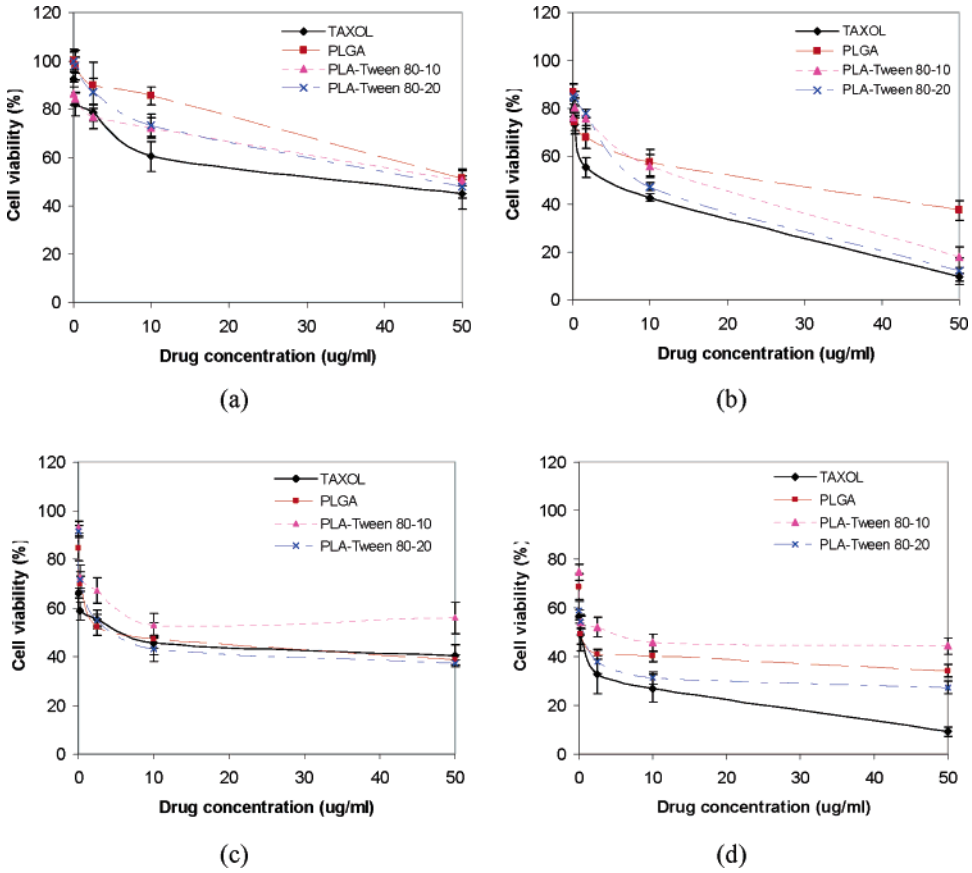

Figure 7. Cytotoxicity of Taxol and paclitaxel-loaded nanoparticles of PLGA and PLA−Tween 80 copolymers, which were incubated with (a) C6 cells for 24 h; (b) C6 cells for 72 h; (c) HT-29 cells for 24 h; and (d) HT-29 cells for 72 h ($n = 6$).

viability was decreased from 37.4 ± 4.0% for the PLGA nanoparticles to 17.8 ± 4.2% for the PLA−Tween 80−10 nanoparticles and 12.0 ± 5.4% for the PLA−Tween 80−20 nanoparticles, which were comparable with that for the free drug, i.e., 9.5 ± 1.6% after incubating with C6 cells for 72 h at the same 50 μg/mL drug concentration ($p > 0.05$). It can be seen from the in vitro drug release profile, however, that the drugs released from the PLA−Tween 80−20 copolymer nanoparticles are only 26.1 ± 4.0% and 39.5 ± 4.7% of encapsulated drug in 24 and 72 h, respectively. The nanoparticles thus should have much better effects in cell cytotoxicity compared with commercial drug formulation.

The similar results for HT-29 cells can be seen from Figure 7, panels c and d. After 24 h incubation, the PLA−Tween 80−20 nanoparticles showed a little higher cytotoxicity (cell viability 37.2 ± 1.5%) compared with that for the free drug (cell viability 40.4 ± 4.6%) at the same drug concentration 50 μg/mL ($p > 0.05$). The PLA−Tween 80−20 copolymer nanoparticles also showed lower cell viability in comparison with the PLGA nanoparticles after being incubated with HT-29 cells for 72 h ($p < 0.05$), which may be explained by faster drug release and smaller particle sizes of the PLA−Tween 80−20 nanoparticles than the PLGA nanoparticles.

4. Conclusion

Novel PLA−Tween 80 copolymers with 8.5% and 15.3% Tween 80 composition were synthesized in this research, and PLA−Tween 80 nanoparticles were prepared by the dialysis method without any other surfactant/emulsifier involved. Paclitaxel was chosen as a prototype anticancer drug due to its excellent therapeutic effects against a wide spectrum of cancers. The nanoparticles were found by FESEM and AFM of spherical shape and around 140 nm in diameter. The copolymers can encapsulate 4.7 ± 0.3% drug in the nanoparticles and release 62 ± 4.2% of the encapsulated drug after 21 days. The drug-loaded PLA−Tween 80 nanoparticles showed in vitro cancer cytotoxicity for HT-29 and G6 cells, which is comparable with that for Taxol at the same drug concentration. However, the effects of the nanoparticle formulation should actually be better with their controlled release feature considered. The PLA−Tween 80 copolymer nanoparticles with higher Tween 80 content (15.3%) in the copolymers showed advantages in in vitro drug release and cytotoxicity in comparison with the PLGA nanoparticles. Further in vivo investigations, such as pharmacokinetics, biodistribution, and xenograft, will be carried out to evaluate the potentials of the copolymer nanoparticles as drug delivery vehicles.

Acknowledgment. This research was supported by NUS Grant R-379-000-014-112, National University of Singapore (S.-S.F., PI) and Singapore Cancer Syndicate (SCS) Grant UU0028 (NUS R397-000-606-305, 2004 and R279-000-187-305, 2005) (SS Feng, PI). Z.P.Z. is grateful to National University of Singapore for the financial support for his Ph.D. study. The authors are grateful to final year project (FYP) student Ng Huibin, Daphne, and MEng student Lee Sie Huey for their assistance in experiments.

References and Notes

(1) Panagi, Z.; Beletsi, A.; Evangelatos, G.; Livaniou, E.; et al. *Int. J. Pharm.* **2001**, *221*, 143−152.
(2) De Jaeghere, F.; Allemann, E.; Feijen, J.; Kissel, T.; et al. *J. Drug Target* **2000**, *8*, 143−153.
(3) Dunn, S. E.; Coombes, A. G. A.; Garnett, M. C.; Davis, S. S.; et al. *J. Controlled Release* **1997**, *44*, 65−76.

(4) Dellacherie, E.; Gref, R.; Quellec, P. *M S-Med. Sci.* **2001**, *17*, 619−626.
(5) Gref, R.; Minamitake, Y.; Peracchia, M. T.; Trubetskoy, V.; et al. *Science* **1994**, *263*, 1600−1603.
(6) Kreuter, J. *Adv. Drug Delivery Rev.* **2001**, *47*, 65−81.
(7) Ramge, P.; Unger, R. E.; Oltrogge, J. B.; Zenker, D.; et al. *Eur. J. Neurosci.* **2000**, *12*, 1931−1940.
(8) Wahab, B. A. A.; Petrov, V. E.; Trofimov, S. S.; Voronina, T. T.; et al. *Eur. Neuropsychopharmacol.* **2005**, *15*, S213−S214.
(9) Dong, Y. C.; Feng, S. S. *Biomaterials* **2005**, *26*, 6068−6076.
(10) Win, K. Y.; Feng, S. S. *Biomaterials* **2005**, *26*, 2713−2722.
(11) Das, D.; Lin, S. S. *J. Pharm. Sci.* **2005**, *94*, 1343−1353.
(12) Sun, W. Q.; Xie, C. S.; Wang, H. F.; Hu, Y. *Biomaterials* **2004**, *25*, 3065−3071.
(13) Koziara, J. M.; Lockman, P. R.; Allen, D. D.; Mumper, R. J. *Pharm. Res.* **2003**, *20*, 1772−1778.
(14) Kreuter, J.; Shamenkov, D.; Petrov, V.; Ramge, P.; et al. *J. Drug Target* **2002**, *10*, 317−325.
(15) Calvo, P.; Gouritin, B.; Chacun, H.; Desmaele, D.; et al. *Pharm. Res.* **2001**, *18*, 1157−1166.
(16) Kharkevich, D.; Alyautdin, R.; Petrov, V.; Ramge, P.; et al. *Naunyn-Schmiedebergs Arch. Pharmacol.* **1998**, *358*, R78−R78.
(17) Alyautdin, R. N.; Tezikov, E. B.; Ramge, P.; Kharkevich, D. A.; et al. *J. Microencapsul.* **1998**, *15*, 67−74.
(18) Schroder, U.; Sabel, B. A. *Brain Res.* **1996**, *710*, 121−124.
(19) Gulyaev, A. E.; Gelperina, S. E.; Skidan, I. N.; Antropov, A. S.; et al. *Pharm. Res.* **1999**, *16*, 1564−1569.
(20) Goppert, T. M.; Muller, R. H. *J. Drug Target* **2003**, *11*, 225−231.
(21) Kim, B. D.; Na, K.; Choi, H. K. *Eur. J. Pharm. Sci.* **2005**, *24*, 199−205.
(22) Pietkiewicz, J.; Sznitowska, M. *Pharmazie* **2004**, *59*, 325−326.
(23) Trotta, M.; Cavalli, R.; Chirio, D. *STP Pharma Sci.* **2003**, *13*, 423−426.
(24) Gref, R.; Domb, A.; Quellec, P.; Blunk, T.; et al. *Adv. Drug Delivery Rev.* **1995**, *16*, 215−233.
(25) Gref, R.; Luck, M.; Quellec, P.; Marchand, M.; et al. *Colloid Surf. B−Biointerfaces* **2000**, *18*, 301−313.
(26) Dong, Y. C.; Feng, S. S. *Biomaterials* **2004**, *25*, 2843−2849.
(27) Avgoustakis, K.; Beletsi, A.; Panagi, Z.; Klepetsanis, P.; et al. *J. Controlled Release* **2002**, *79*, 123−135.
(28) Ryu, J. G.; Jeong, Y. I.; Kim, Y. H.; Kim, I. S.; et al. *Bull. Korean Chem. Soc.* **2001**, *22*, 467−475.
(29) Sakurai, K.; Nakada, Y.; Nakamura, T.; Tudomi, R.; et al. *J. Macromol. Sci.-Pure Appl. Chem.* **1999**, *36*, 1863−1877.
(30) Ha, J. C.; Kim, S. Y.; Lee, Y. M. *J. Controlled Release* **1999**, *62*, 381−392.
(31) Zhang, Z. P.; Feng, S. S. *Biomaterials* **2006**, *27*, 262−270.
(32) Donehower, R. C.; Rowinsky, E. K.; Grochow, L. B.; Longnecker, S. M. *Cancer Treatment Rep.* **1987**, *71*, 1171−1177.
(33) Kohler, D. R.; Goldspiel, B. R. *Pharmacotherapy* **1994**, *14*, 3−34.
(34) Lopes, N. M.; Adams, E. G.; Pitts, T. W.; Bhuyan, B. K. *Cancer Chemother. Pharmacol.* **1993**, *32*, 235−242.
(35) Spencer, C. M.; Faulds, D. *Drugs* **1994**, *48*, 794−847.
(36) Fjallskog, M. L.; Frii, L.; Bergh, J. *Lancet* **1993**, *342*, 873−873.
(37) Gelderblom, H.; Verweij, J.; Nooter, K.; Sparreboom, A. *Eur. J. Cancer* **2001**, *37*, 1590−1598.
(38) Panchagnula, R. *Int. J. Pharm.* **1998**, *172*, 1−15.
(39) van Tellingen, O.; Huizing, M. T.; Panday, V. R. N.; Schellens, J. H. M.; et al. *Br. J. Cancer* **1999**, *81*, 330−335.
(40) Weiss, R. B.; Donehower, R. C.; Wiernik, P. H.; Ohnuma, T.; et al. *J. Clin. Oncol.* **1990**, *8*, 1263−1268.
(41) Mu, L.; Feng, S. S. *J. Controlled Release* **2003**, *86*, 33−48.
(42) Mu, L.; Feng, S. S. *Pharm. Res.* **2003**, *20*, 1864−1872.
(43) Mu, L.; Feng, S. S. *J. Controlled Release* **2002**, *80*, 129−144.
(44) Xiong, X. Y.; Tam, K. C.; Gan, L. H. *Macromolecules* **2003**, *36*, 9979−9985.
(45) Moghimi, S. M.; Hunter, A. C., Murray, J. C. *Pharmacol. Rev.* **2001**, *53*, 283−318.
(46) Seymour, L. W. *Crit. Rev. Theory Drug Carrier Syst.* **1992**, *9*, 135−187.
(47) Chen, Y.; Dalwadi, G.; Benson, H. A. E. *Curr. Drug Delivery* **2004**, *1*, 361−376.
(48) Scholes, A. G. A. C.; Illum, L.; David, S. S.; Watts, J. F.; et al. *J. Controlled Release* **1999**, *59*, 261−278.
(49) Peracchia, M. T.; Gref, R.; Minamitake, Y.; Domb, A.; et al. *J. Controlled Release* **1997**, *46*, 223−231.
(50) Stolnik, S.; Garnett, M. C.; Davies, M. C.; Illum L.; et al.*Colloids Surf. A: Physicochem. Eng. Aspects* **1995**, *97*, 235−245.

BM050953V